patients with lung adenocarcinomas (Table 3). No significant associations were observed between p16 HDs and gender, age, and smoking history in all 50 cases analyzed (Table 3), as well as in 28 cases of primary adenocarcinomas or in 22 cases of brain metastases (data not shown). p16 HDs were not associated with pathologic stage nor with 5-year survival in 28 cases of primary adenocarcinomas (Table 3). Previously, p16 methylation was shown to be associated with smoking history (1, 7). Thus, no association of p16 HDs with smoking history was in contrast with the status of p16 methylation in lung adenocarcinomas. The results indicate that causative factors for p16 HD were different from those for p16 methylation, although both alterations result in the inactivation of the same gene. Previously, Kraunz and colleagues reported that p16 HD occurred at a higher frequency in never-smokers as compared with former and current smokers (6). Although such an association was not observed in this study, both studies indicated the absence of a positive association between p16 HD and smoking history, and the possible association of p16 HD with other causative factors for lung adenocarcinoma. Thus, further studies are needed for the elucidation of such factors because little is known about the environmental as well as genetic risk factors for lung adenocarcinoma. The absence of any association between p16 HDs and 5-year survival was also in contrast with the status of p16 methylation in lung adenocarcinomas. However, because the number of cases examined was small (28 cases), and the patients with poor prognosis had a higher frequency of p16 HDs than those with good prognosis (44% versus 21%), further studies will be required on this subject. The absence of any association between p16 HDs and pathologic stage further supports their occurrence in the early stages, rather than in the late stages, of lung adenocarcinoma progression.

Association of p16 HDs with EGFR, KRAS, and p53 mutations. We next evaluated the association of p16 HDs with the status of EGFR, KRAS, and p53 mutations in these samples (Tables 1 and 3). Then, based on the results of these molecular analyses and a previous p16 methylation analysis (7), a stepwise malignant progression model for small-sized lung adenocarcinoma was depicted as shown in Fig. 4. As previously reported (14, 18), EGFR and KRAS mutations were detected in a mutually exclusive manner in lung adenocarcinomas. EGFR mutations were most frequently detected in type B tumors (8 of 8, 100%), suggesting the involvement of EGFR mutations in the formation of noninvasive BACs. Although KRAS mutations were detected only in type C and D tumors in this study, it was recently reported that the mutations were frequently detected in noninvasive adenocarcinomas and also in atypical adenomatous hyperplasias (AAH; ref. 19). Thus, it is likely that either EGFR or KRAS mutations occur prior to HDs and methylations of the p16 gene in the progression of BACs, although it is also possible that p16 alterations occur earlier than depicted in Fig. 4. Frequencies of p53 mutations in primary adenocarcinomas were the highest in type D (5 of 5, 100%), intermediate in type C (9 of 15, 60%), and the lowest in type B (2 of 8, 25%), suggesting the accumulation of the mutations during progression from noninvasive adenocarcinomas to invasive ones. Thus, it was likely that p53 mutations had accumulated in adenocarcinomas with p16 HDs and/or EGFR/KRAS mutations. It is indispensable to analyze a considerable number of AAHs as well as type A tumors to fully understand the timing of each genetic alteration in sequential progression of lung adenocarcinomas because AAH is a putative precursor of peripheral lung adenocarcinoma including BAC (20), and sequential progression from type A to type C tumors through type B tumors was strongly indicated in previous

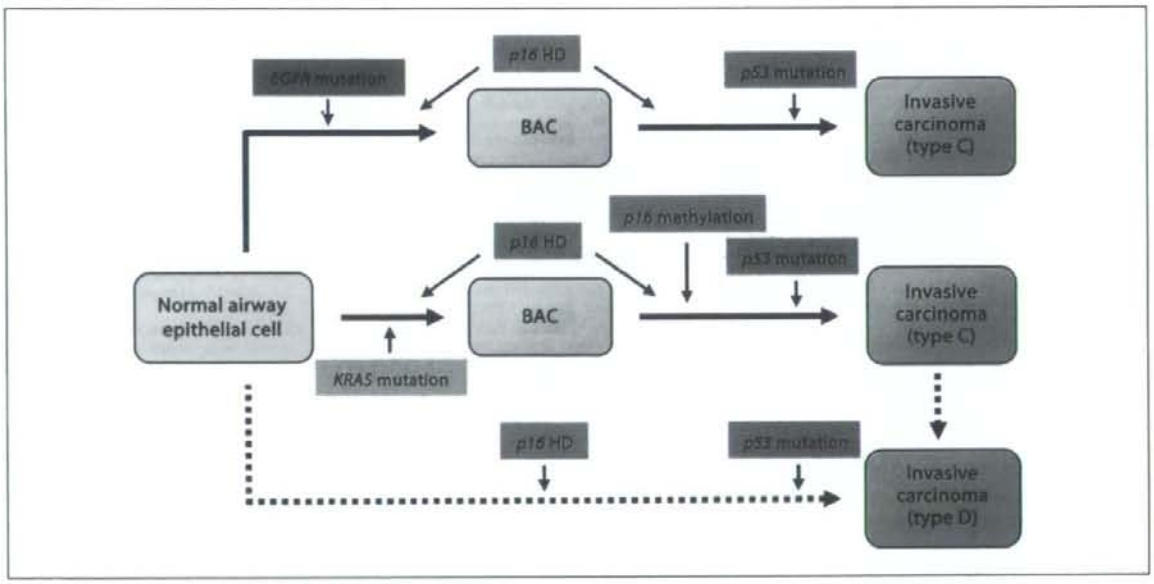

Fig. 4. A stepwise malignant progression model of small-sized lung adenocarcinoma in association with accumulated genetic alterations in cells. BAC, bronchioloalveolar carcinoma; type C, localized bronchioloalveolar carcinoma with foci of active fibroblastic proliferation; type D, poorly differentiated adenocarcinoma.

studies (7, 21). However, because AAH is not routinely resected by surgery and because type A tumors are usually very small, the number of tumors as well as the amount of DNA obtained was not enough for the present study.

There was no specificity for the occurrence of p16 HDs among adenocarcinomas with regard to other accompanied genetic alterations. In particular, p16 HDs were detected with similar frequencies (17–29%), irrespective of the presence or absence of EGFR, KRAS, and p53 mutations (Table 3). This result indicates that p16 HDs occur with similar frequencies in EGFR type as well as KRAS type and non-EGFR/KRAS type adenocarcinomas. In this model, type C tumors were considered to progress from BACs, as previously indicated by Aoyagi and colleagues (21). However, it was still unclear whether type D tumors arise *de novo* by a distinct pathway from tumors with BAC components or progress from these tumors. Low frequencies of EGFR mutations and high frequencies of p53 mutations in type D tumors indicate that type D tumors progress from either the KRAS types or non-EGFR/KRAS types. Haneda and colleagues also reported a low frequency of EGFR mutations in type D tumors (22), supporting the presence of a non-EGFR pathway for the development of type D poorly differentiated adenocarcinomas.

Conclusions. MLPA analysis of microdissected small-sized primary adenocarcinoma cells revealed that p16 HDs are present in 20% to 40% of adenocarcinomas irrespective of the presence of mutations in the *EGFR*, *KRAS*, and *p53* genes, and occur early in the development of lung adenocarcinomas. HDs were not associated with smoking history of the patients. It has been indicated that smoking is a major factor inducing p16 methylation as well as KRAS mutation. In contrast, EGFR mutations frequently occur in female nonsmokers and are associated with bronchioloalveolar morphology of adenocarcinomas. Interestingly, p16 HDs did not coexist with specific genetic alterations in adenocarcinoma cells. Thus, causative factors for p16 HD would be different from those for p16 methylation, KRAS mutations, and EGFR mutations. To elucidate the causative role for the occurrence of p16 HDs in multistage lung carcinogenesis, further studies should focus on the identification of environmental and genetic factors for the induction of DNA double-strand breaks surrounding the *p16* gene locus and their repair systems.

Disclosure of Potential Conflicts of Interest

No potential conflicts of interest were disclosed.

Acknowledgments

We thank Drs. Higashi and Yokoyama of FALCO Biosystems, Ltd., for their technical support and critical discussion in MLPA analysis. We also thank Drs. Nakanishi and Matsumoto for the laser capture microdissection of cancer cells from primary small-sized lung adenocarcinomas.

References

1. Toyooka S, Tokumo M, Shigematsu H, et al. Mutational and epigenetic evidence for independent pathways for lung adenocarcinomas arising in smokers and never smokers. Cancer Res 2006;66:1371–5.
2. Sato M, Shames DS, Gazdar AF, Minna JD. A translational view of the molecular pathogenesis of lung cancer. J Thorac Oncol 2007;2:327–43.
3. Hamada K, Kohno T, Kawanishi M, Ohwada S, Yokota J. Association of CDKN2A(p16)/CDKN2B(p15) alterations and homozygous chromosome arm 9p deletions in human lung carcinoma. Genes Chromosomes Cancer 1998;22:232–40.
4. Sanchez-Cespedes M, Reed AL, Buta M, et al. Inactivation of the INK4A/ARF locus frequently coexists with TP53 mutations in non-small cell lung cancer. Oncogene 1999;18:5843–9.
5. Sanchez-Cespedes M, Decker PA, Doffek KM, et al. Increased loss of chromosome 9p21 but not p16 inactivation in primary non-small cell lung cancer from smokers. Cancer Res 2001;61:2092–6.
6. Kraunz KS, Nelson HH, Lemos M, Godleski JJ, Wiencke JK, Kelsey KT. Homozygous deletion of p16INK4a and tobacco carcinogen exposure in non-small cell lung cancer. Int J Cancer 2006;118:1364–9.
7. Tanaka R, Wang D, Morishita Y, et al. Loss of function of p16 gene and prognosis of pulmonary adenocarcinoma. Cancer 2005;103:608–15.
8. Chen JT, Chen YC, Wang YC, Tseng RC, Chen CY, Wang YC. Alterations of the p16(ink4a) gene in resected nonsmall cell lung tumors and exfoliated cells within sputum. Int J Cancer 2002;98:724–31.
9. Schouten JP, McElgunn CJ, Waaijer R, Zwijnenburg D, Diepvens F, Pals G. Relative quantification of 40 nucleic acid sequences by multiplex ligation-dependent probe amplification. Nucleic Acids Res 2002;30:e57.
10. Worsham MJ, Chen KM, Tiwari N, et al. Fine-mapping loss of gene architecture at the CDKN2B (p15INK4b), CDKN2A (p14ARF, p16INK4a), and MTAP genes in head and neck squamous cell carcinoma. Arch Otolaryngol Head Neck Surg 2006;132:409–15.
11. Mistry SH, Taylor C, Randerson-Moor JA, et al. Prevalence of 9p21 deletions in UK melanoma families. Genes Chromosomes Cancer 2005;44:292–300.
12. Sobin LH, Wittekind CH, editors. TNM classification of malignant tumours. 6th ed. New York: Wiley-Liss; 2002. p. 99–103.
13. Noguchi M, Morikawa A, Kawasaki M, et al. Small adenocarcinoma of the lung. Histologic characteristics and prognosis. Cancer 1995;75:2844–52.
14. Matsumoto S, Iwakawa R, Kohno T, et al. Frequent EGFR mutations in noninvasive bronchioloalveolar carcinoma. Int J Cancer 2006;118:2498–504.
15. Sakamoto H, Mori M, Taira M, et al. Transforming gene from human stomach cancers and a noncancerous portion of stomach mucosa. Proc Natl Acad Sci U S A 1986;83:3997–4001.
16. Matsumoto S, Takahashi K, Iwakawa R, et al. Frequent EGFR mutations in brain metastases of lung adenocarcinoma. Int J Cancer 2006;119:1491–4.
17. Hamada K, Kohno T, Takahashi M, et al. Two regions of homozygous deletion clusters at chromosome band 9p21 in human lung cancer. Genes Chromosomes Cancer 2000;27:308–18.
18. Riely GJ, Politi KA, Miller VA, Pao W. Update on epidermal growth factor receptor mutations in non-small cell lung cancer. Clin Cancer Res 2006;12:7232–41.
19. Sakamoto H, Shimizu J, Horio Y, et al. Disproportionate representation of KRAS gene mutation in atypical adenomatous hyperplasia, but even distribution of EGFR gene mutation from preinvasive to invasive adenocarcinomas. J Pathol 2007;212:287–94.
20. Travis WD, Brambilla E, Muller-Hermelink HK, Harris CC, editors. Pathology and genetics: tumours of the lung, pleura, thymus and heart. Lyon: IARC Press; 2004. p. 73–5.
21. Aoyagi Y, Yokose T, Minami Y, et al. Accumulation of losses of heterozygosity and multistep carcinogenesis in pulmonary adenocarcinoma. Cancer Res 2001;61:7950–4.
22. Haneda H, Sasaki H, Shimizu S, et al. Epidermal growth factor receptor gene mutation defines distinct subsets among small adenocarcinomas of the lung. Lung Cancer 2006;52:47–52.

Journal of Pathology
J Pathol 2008; **216**: 75–82
Published online 13 May 2008 in Wiley InterScience
(www.interscience.wiley.com) **DOI:** 10.1002/path.2383

Original Paper

Expression profile of early lung adenocarcinoma: identification of *MRP3* as a molecular marker for early progression

S Hanada,[1,5] A Maeshima,[2,7] Y Matsuno,[2,6] T Ohta,[1] M Ohki,[1] T Yoshida,[1,3] Y Hayashi,[4] Y Yoshizawa,[5] S Hirohashi[2] and M Sakamoto[2,4]*

[1]*Center for Medical Genomics, National Cancer Center Research Institute, Tokyo, Japan*
[2]*Pathology Division, National Cancer Center Research Institute, Tokyo, Japan*
[3]*Genetic Division, National Cancer Center Research Institute, Tokyo, Japan*
[4]*Department of Pathology, Keio University School of Medicine, Tokyo, Japan*
[5]*Department of Integrated Pulmonology, Tokyo Medical and Dental University, Tokyo, Japan*
[6]*Department of Surgical Pathology, Hokkaido University Hospital, Hokkaido, Japan*
[7]*Clinical Laboratory Division, National Hospital Organization Tokyo Medical Center, Tokyo, Japan*

*Correspondence to:
M Sakamoto, Department of Pathology, Keio University School of Medicine, 35 Shinanomachi, Shinjuku-ku, Tokyo 160-0016, Japan.
E-mail: msakamot@sc.itc.keio.ac.jp

No conflicts of interest were declared.

Abstract

Early lung adenocarcinoma is well-recognized as a small-sized non-invasive adenocarcinoma or localized non-mucinous bronchioloalveolar carcinoma (LNMBAC); however, the molecular events associated with these early lesions are not clear. To determine the genes involved in tumorigenesis at the early stage of lung adenocarcinoma, we compared the mRNA expression profiles of LNMBAC and normal lungs with an oligonucleotide array. Immunohistochemical analyses were performed to confirm the expression of detected genes. We identified 183 differentially expressed genes, of which 15 were up-regulated and 168 down-regulated. Among them, most up-regulated genes, such as *AQP3* and *Claudin-4*, were expressed in both adenocarcinoma cells and type II alveolar pneumocytes, corresponding to the histological similarity between these cell types. However, multidrug resistant protein 3 (MRP3) was only expressed on tumour cell membranes and not in type II alveolar pneumocytes, as confirmed by immunohistochemistry. Moreover, the number of MRP3-positive cells significantly increased from AAH (the precursor lesion of lung adenocarcinoma) to LNMBAC. We conclude that MRP3 could be a novel molecular marker for LNMBAC, whose expression increases during the early progression of tumourigenesis.

Keywords: lung adenocarcinoma; localized non-mucinous BAC (LNMBAC); expression profile; microarray; MRP3

Received: 26 February 2008
Revised: 30 April 2008
Accepted: 5 May 2008

Introduction

Lung cancer is the leading cause of death in western countries and Japan. Among the four major histological types, adenocarcinoma is the most common, with the number of afflicted patients increasing in recent years. As lung adenocarcinomas are usually detected late in disease progression and are recalcitrant to morphological and molecular analyses, owing to their histological and cytological heterogeneity, the molecular mechanisms of adenocarcinoma tumourgenesis remain relatively unknown, especially in the early stage [1].

Introduction of high-resolution computed tomography (HRCT) to lung cancer diagnosis has made it possible to detect atypical adenomatous hyperplasia (AAH), a presumed precursor lesion or peripheral small-sized adenocarcinoma that can hardly be detected by X-ray examination [2–6]. Early lung adenocarcinoma is a novel concept and category derived from the clinicopathological analysis of small peripheral lung adenocarcinomas. Thus, this category is different from early cancer, which usually indicates stage I lung adenocarcinomas of the TMN classification. Noguchi *et al* histopathologically examined small adenocarcinomas (<2 cm) and subdivided them into two groups; those having a replacing growth structure and those having a non-replacing and destructive structure [7]. The former group includes three types: type A, a localized bronchioloalveolar carcinoma (LBAC); type B, comprised of LBAC with alveolar collapse; and type C, LBAC with active fibroblastic change. Because type A and type B adenocarcinomas, which are localized non-mucinous BAC (LNMBAC) in the World Health Organization (WHO) classification, have

no interstitial invasion, no lymph node metastasis, and their 5 year survival rates are 100%, they are categorized as early lung adenocarcinomas.

According to recent studies, the progression of lung adenocarcinoma is considered to be caused by sequential molecular events like the adenoma–carcinoma sequence of colon cancer [8]. Studying LNMBAC could be a great help in elucidating the first step of the sequential molecular events underlying tumourigenesis. Although several studies have reported molecular events involving K-ras or P53 for small adenocarcinoma or AAH, most of the molecular mechanisms of the early stage remain unclear [9–11]. Understanding the probability and interval of clinical progression from AAH to overt malignancy, as well as from early to advanced adenocarcinoma, would also be very useful for clinical management. Novel tumour markers for early adenocarcinoma may help to diagnose LNMBAC more objectively.

The microarray technique is a recently developed and powerful tool for examining the expression of a massive number of genes at one time and has proved useful in the characterization of cancers [12–14]. In the present study, to determine molecular events and to find genes that characterize early lung adenocarcinoma, we compared the gene expression of LNMBAC and normal lungs with the oligonucleotide microarray. We identified a gene set that distinguished the tumour from the normal lung and specifically found that MRP3 expression increased during the early progression of tumourigenesis, suggesting its utility as a novel molecular marker for early lung adenocarcinoma.

Materials and methods

Tissue samples

Ten lung adenocarcinomas and 10 normal lungs were obtained from patients who underwent surgical resection at National Cancer Centre Hospital, Japan, and the study was approved by the National Cancer Centre ethics review board. Of the samples, four were paired tumours and corresponding non-cancerous lung tissue from the same patients. First, small samples for molecular analysis were obtained from surgically resected specimens and immediately cut into small pieces, snap-frozen in liquid nitrogen and stored until use. The the rest of the whole resected specimens were fixed routinely in 10% formalin, cut serially into 5–7 mm slices, and macroscopically examined. From the section including the largest diameter of the tumour, all the tumour tissue as well as the surrounding lung tissue was removed and embedded in paraffin, and then cut into 4 μm sections. Haematoxylin and eosin (H&E) and elastica and Van Gieson (EVG) staining was performed. All tumours were <3 cm in diameter (range 0.7–2.7 cm) and histologically diagnosed as LNMBAC without active fibroblastic change by two individual pathologists (Figure 1 and Table 1). For immunohistochemical analysis, 15 normal lungs, 10 hyperplasias, 15 AAHs and 12 LNMBACs were analysed. Sections were prepared from formalin-fixed, paraffin-embedded tissues of surgically resected samples.

Microarray analysis

For gene expression analysis, we used the GeneChip human Genome HG-U95Av2 oligonucleotide microarray (Affymetrix, Santa Clara, CA, USA). Target cRNA for microarray hybridization was prepared as follows. Total RNA was isolated using RNeasy columns (Qiagen, Hilden, Germany) according to the manufacturer's instructions. From 5 μg total RNA, double-stranded cDNA with a T7 promoter tag was generated using the Superscript Choice system (Invitrogen), and biotin-labelled cRNA was synthesized from the double-stranded cDNA by *in vitro* transcription, using a BioArray RNA transcript-labelling kit (Enzo Diagnostics, Farmingdale, NY, USA). The cRNA was purified using RNeasy columns; 20 μg biotin-labelled cRNA was fragmented at 94 °C for 35 min in 40 μl 1× RNA fragmentation buffer (40 mM Tris/acetate, pH 8.1, 100 mM K acetate and 30 mM Mg acetate) and used for microarray hybridization. Hybridization, washing, staining, and scanning were carried out according to the manufacturer's instructions. Briefly, 10 μg biotin-labelled and fragmented cRNA was hybridized to the microarray in 200 μl 1× 4-morpholinepropanesulphonic acid (MES) hybridization buffer (100 mM MES/Na-MES, pH 6.6, 890 mM NaCl, 20 mM EDTA, 0.01% Tween 20) containing 0.1 mg/ml herring sperm DNA (Promega, Madison, WI, USA) and 0.5 mg/ml acetylated BSA (Invitrogen) at 45 °C for 16 h with rotation. Subsequently,

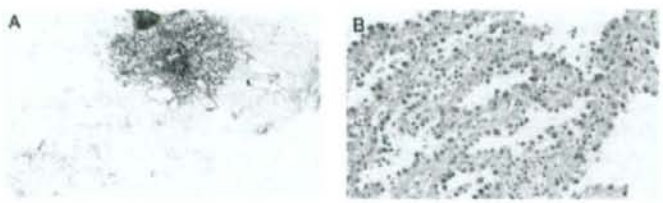

Figure 1. Histology of early lung adenocarcinoma (LNMBAC). The boundary between the tumour and the surrounding normal lung is indistinct. Each tumour cell resembles a type II pneumocyte and grows by replacing alveolar lining cells (H&E original magnification, ×400)

the microarrays were washed with non-stringent wash buffer (60 mM Na_2HPO_4/NaH_2PO_4, pH 7.4, 894 mM NaCl, 6 mM EDTA and 0.01% Tween 20) at 25 °C and then with stringent wash buffer (100 mM MES/Na-MES, pH 6.6 26 mM NaCl and 0.01% Tween 20) at 50 °C, stained with streptavidin–phycoerythrin (Molecular Probes) and biotinylated antistreptavidin (Vector Laboratories, Burlingame, CA, USA) and scanned with a GeneArray scanner (Hewlett-Packard, Santa Clara, CA, USA).

Data analysis

Using the Microarray Suite 4.0 software package (Affymetrix), scanned images were transformed into signals called the average difference, which represented the mean difference of signal intensities between match and mismatch probe pairs. The hybridization intensities were normalized to 1000 across all samples. Data analyses were done using Excel (Microsoft), GeneSpring (Silicon Genetics, Redwood City, CA, USA) and Cluster (Stanford) and visualized using Tree and View (Stanford).

RT–PCR

From the total RNA samples, template cDNA was synthesized with an oligo(dT) primer and Super Script Choice System (Invitrogen). PCR was performed with AmpliTaq Gold and the GeneAmp 7700 Sequence Detector (Applied Biosystems, Foster City, CA, USA). The primer sets for MRP3 were designed as 5′-CTGCTAAACCCTGACCCTCTGCGG-3′ (forward) and 5′-TCCAGCAGCTGCTGCACCACCATC-3′ (reverse). PCR conditions were as follows: 1 cycle at 94 °C for 10 min, then 30 cycles at 95 °C for 15 s, 60 °C for 1 min and 75 °C for 30 °C, followed by a final 75 °C extension for 10 min. For standardization of the amount of RNA, expression of glyceraldehyde 3-phosphate dehydrogenase (GAPDH) was quantified for each sample.

Immunohistochemistry

Immunohistochemistry was performed on formalin-fixed, paraffin-embedded tissue sections by an immunoperoxidase method, as described previously [15]. Antibodies used for immunohistochemical analysis were MRP3 (M3II-21; Signet Laboratories Inc., MA, USA) at a dilution of 1 : 100, TTF-1 (Neomarkers, Fremont, CA, USA) at a dilution of 1 : 200, AQP3 (Santa Cruz Biotechnology, Santa Cruz, CA, USA) at a dilution of 1 : 200, and Claudin-4 (Zymed Laboratories, South San Francisco, CA, USA) at a dilution of 1 : 200.

Staining evaluation

Staining was evaluated by two independent observers. The positivity index was expressed as the percentage of positive cells in each lesion.

Results

Gene expression profiling of LNMBAC

To identify genes that characterized early lung adenocarcinoma, we compared expression profiles between 10 LNMBACs and 10 normal lungs, using the oligonucleotide array. We applied two independent types of supervised analysis.

The first analysis proceeded using the following criteria. (a) Genes whose average differences (mean difference in signal intensity between perfect match and mismatch probe pairs) were >1000 in at least 5/20 samples. (b) *t*-Test with significance set at $p < 0.05$ to identify genes expressed differently between tumours and normal tissue. (c) Multiple testing corrections (Young and permutation test) applied by Gene Spring software. Multiple testing correction adjusts the individual p value for each gene to keep the overall error rate to less than or equal to the specific p value cut-off. Using these criteria, we selected 183 differentially expressed genes from 12 696 probe sets, 15 genes that were up-regulated in tumours (Table 2) and 168 down-regulated genes (Supplementary Table 1, available at: http://www.interscience.wiley.com/jpages/0022-3417/suppmat/path.2383.html). To validate that these genes could actually distinguish early adenocarcinomas from normal lungs, we applied hierarchical clustering to classify the same sample sets, using the 183 selected genes (Figure 2).

The second analysis proceeded using the following criteria. (a) Presence in tumours (i.e. exactly

Table 1. Clinicopathological feature of surgically resected specimens

Patient No.	Gender	Age	Stage	T	N	M	Histological differentiation	Vascular invasion	Lympho duct invasion	Smoking		Brinkman index
K186	F	61	IA	1	0	0	Well	–	–	+	Current	375
K187	M	55	IA	1	0	0	Well	–	–	+	Current	700
K230	F	66	IA	1	0	0	Well	–	–	–	Never	
K228	F	69	IA	1	0	0	Well	–	–	+	Current	165
K236	F	73	IA	1	0	0	Well	–	–	–	Never	
K265	M	76	IA	1	0	0	Well	–	–	+	Former	450
K269	M	52	IA	1	0	0	Well	–	–	+	Current	640
K274	M	59	IA	1	0	0	Well	–	–	+	Former	360
K303	M	65	IA	1	0	0	Well	–	–	–	Never	

Table 2. List of genes up-regulated in LNMBAC compared to normal lungs

Symbol	Affymetrix probe No.	p Value	Locus	Gene description
ABCC3	1930_at	0.016	17q22	ATP-binding cassette, sub-family C (CFTR/MRP), member 3
WFDC2	33933_at	0.001	20q12–q13.2	WAP four-disulphide core domain 2
AQP3	39248_at	0.003	9p13	Aquaporin 3
ADAM8	40712_at	0.021	10q26.3	A disintegrin and metalloproteinase domain 8
CACNB1	36557_at	0.024	17q21–q22	Calcium channel, voltage-dependent, β 1 subunit
MST1R	1317_at	0.028	3p21.3	Macrophage stimulating 1 receptor (c-met-related tyrosine kinase)
BENE	33331_at	0.032	2q13	BENE protein
CLDN4	35276_at	0.001	7q11.23	Claudin 4
KIAA0907	33885_at	0.026	1q21.2	KIAA0907 protein
KIAA0657	35780_at	0.013	2q36.3	KIAA0657 protein
GCN5L2	38628_at	0.003	17q21	GCN5 general control of amino-acid synthesis 5-like 2 (yeast)
CHC1	1196_at	0.009	1p36.1	Chromosome condensation 1
LGALS3BP	37754_at	0.003	17q25	Lectin, galactoside-binding, soluble, 3 binding protein
ITPR3	37343_at	0.032	6p21	Inositol 1,4,5-triphosphate receptor, type 3
KIAA0076	36084_at	0.032	6p21.1	KIAA0076 gene product

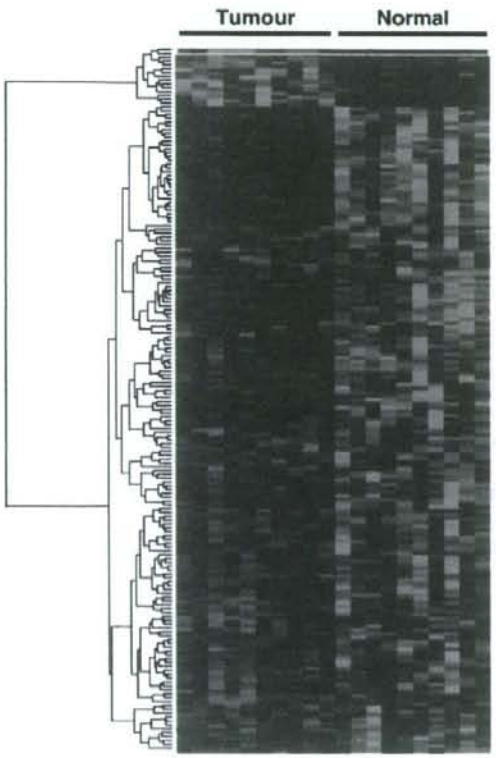

Figure 2. Expression profiling of LNMBAC. Hierarchial clustering was performed, in which 183 differentially expressed genes clearly differentiated LNMBACs from normal lungs. The normalized expression index of each transcript is indicated by a coloured bar. Up-regulated genes were expressed as red and down-regulated genes as green

expressed in the samples). (b) Average difference of >1000. (c) A > three-fold increase in average difference when compared to 10 normal sample mixtures in at least 5/10 samples. Using these criteria, we selected 140 genes that were up-regulated by more than three-fold (Supplementary Table 2, available at: http://www.interscience.wiley.com/jpages/0022-3417/suppmat/path.2383.html).

Genes expressed in both type II alveolar pneumocytes and LNMBAC

For the up-regulated genes listed in Table 2 and Supplementary Table 2, we selected interesting genes and performed immunohistochemical analysis on LNMBACs. We also examined AAH, hyperplasia and normal regions from the surrounding lung.

We examined *TTF-1*, *AQP3* and *Claudin-4* (Figure 3). We also analysed *MST1R* (*RON*), *MUC1*, *CD24*, *HNF1b*, *ARFGEF1*, *GRB7*, *AQP5* and *NQO1* (data not shown); those genes were specifically expressed in tumour cells and could not be detected in the interstitial areas in carcinoma tissue. In surrounding regions, normal type II pneumocytes were also positive in every case, whereas type I cells were negative. The staining intensity of TTF-1 in tumour cells was the same as in normal type II pneumocytes; however, that of AQP3 and Claudin-4 in tumour cells was stronger than in normal type II pneumocytes. In hyperplasia and AAH, these genes were also positive in the type II pneumocytes and atypical cells that morphologically resembled type II pneumocytes, respectively (data not shown). Therefore, these genes were considered to be related to features of type II pneumocytes.

MRP3 expression in LNMBAC

Of the genes listed in Table 2 and Supplemenatry Table 2, *MRP3* was the only one that was up-regulated more than three-fold in all 10 samples as well as being undetectable in the normal lung. (Figure 4) To confirm the mRNA level of *MRP3*, we applied RT–PCR (Figure 5). In all four LNMBACs examined, *MRP3* was up-regulated when compared to the corresponding normal lung tissue, where expression was almost undetectable.

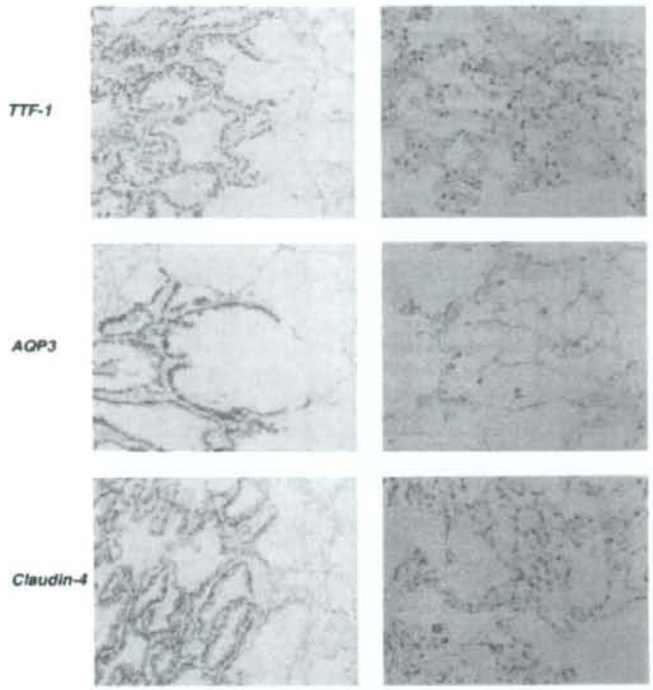

Figure 3. Immunohistochemical analysis of *TTF-1* (top), *AQP3* (middle) and *Claudin-4* (bottom) on LNMBAC (left) and normal lung (right). These genes were specifically expressed in tumour cells and could not be detected in interstitial areas in carcinoma tissue. In surrounding normal regions, histologically normal type II pneumocytes were also positive in every case, whereas type I cells were negative. The staining intensity of TTF-1 in tumour cells and normal type II pneumocytes was the same, while that of AQP3 and Claudin-4 was stronger in tumour cells

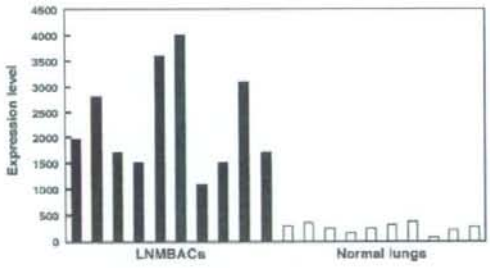

Figure 4. Expression signal of *MRP3* as measured by oligonucleotide microarray. Each bar expresses raw average difference data. All black bars representing the expression signal in LNMBACs indicate a range of about 1000–4000, whereas all white bars representing signals from normal lungs indicate undetectable expression

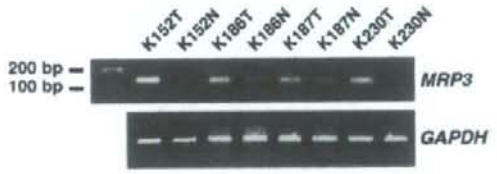

Figure 5. *MRP3* expression in LNMBAC. RT–PCR was performed to confirm the mRNA level of *MRP3* with four paired samples. The expression level of *MRP3* in LNMBAC was up-regulated when compared to that in the corresponding normal lung tissue

To determine whether *MRP3* was also expressed at the protein level, we employed a monoclonal antibody against MRP3 in an immunohistochemical study (Figure 6) and counted positively-stained cells in each lesion (Figure 7). We examined LNMBAC, the surrounding normal lung, hyperplasia and AAH. The immunohistochemical study demonstrated strong expression of MRP3 on cell membranes in LNMBACs, and most LNMBAC samples expressed MRP3 in more than 50% of tumour cells. In normal lung and hyperplasia, including type II pneumocytes, we could not detect MRP3 protein. MRP3 protein expression in AAH varied among samples; however, most samples did not express or scarcely expressed MRP3. The percentage of positive cells increased stepwise according to the progression of lung adenocarcinoma.

Discussion

In this paper we present gene expression profiling of LNMBAC and identify a distinct gene set that distinguishes tumours from normal lung tissue; these

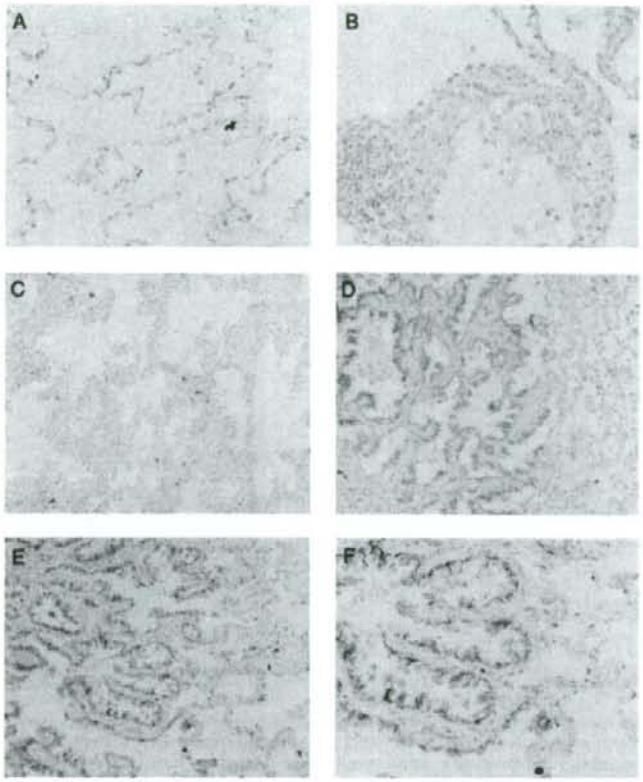

Figure 6. Immunohistochemical evaluation of *MRP3* expression in LNMBAC. Immunohistochemistry demonstrated negative expression in normal lung (A) and hyperplasia (B). Staining was also rarely detectable in AAH (C). *MRP3* expression was observed on the cell membrane in LNMBAC (D) and another case of LNMBAC (E and F). Original magnifications: ×40 (D), ×100 (E) and ×200 (F)

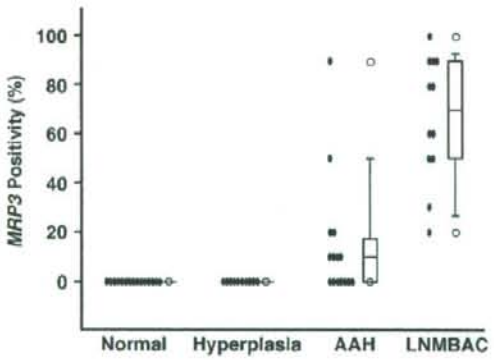

Figure 7. Relationship between immunohistochemical expression of MRP3 and LNMBAC. Scattergram and box plot show the relationship between *MRP3* immunostaining and normal lung, hyperplasia, AAH and LNMBAC. The box encompasses the 25th to 75th percentiles of results obtained, with the 50th percentile representing the median. The 5th and 95th percentiles are shown as white circles, and below and above the circles are 10th and 90th percentile whisker caps, respectively. The percentage of positive cells increased according to the stepwise progression of lung adenocarcinoma

genes particularly characterize LNMBAC. Of the up-regulated genes, we identified *MRP3* as a novel molecular marker for LNMBAC. We also identified novel type II pneumocyte lineage tumour markers.

MRP3 was identified as an up-regulated gene by two independent supervised analyses. The most remarkable feature of *MRP3* was that its expression was detected in tumour cells but not in normal type II pneumocytes. *MRP3* expression increased concomitantly with the stepwise progression from the precursor lesion of lung adenocarcinoma to AAH to LNMBAC. Moreover, *MRP3* was not detected in type II pneumocyte hyperplasia. The border between AAH and LNMBAC is unclear and sometimes varies by pathologist. This diagnostic difficulty generates severe confusion for clinical treatment; the establishment of standard management is of top priority for clinical oncologists. *MRP3* could therefore be a novel objective tumour marker for histological diagnosis and an important marker for lung cancer in the future. Our findings also suggest that *MRP3* might function as a primary factor in carcinogenesis. *MRP3* was found to be an anti-cancer drug-resistant gene in a lung cancer cell line [16]. *MRP3* belongs to the ABC transporter

membrane protein family, and some anti-cancer drugs induce *MRP3* expression to obtain a resistant phenotype [17–21]. However, none of the samples used in this study had received any anti-cancer drug therapy before analysis; therefore the observed *MRP3* expression was not induced by anti-cancer drugs. There is widely accepted view that BAC is less chemosensitive than other non-small cell lung carcinomas; however, this is not clearly supported by scientific evidence [22]. The hypothesis that observed *MRP3* expression in LNMBAC might produce congenital drug resistance would need further study. Recent studies have revealed that *ABCG2/BRCP*, a member of the ABC transporter family, can generate a cancer stem cell phenotype in addition to drug resistance [23,24]. If cancer stem cells also play a role in lung adenocarcinogenesis, then *MRP3* expression might be involved.

Well-established type II pneumocyte markers, such as *KL-6* (*MUC1*) and *SP-D*, are already used in clinical practice to determine the activity of interstitial pneumonia [25]. Upon expression profiling of LNMBAC, we identified several novel type II pneumocyte markers, such as *AQP3*, *RON* and *Claudin-4*, and it is expected that these molecules might also serve as markers for lung pathophysiology. Additionally, these markers were also expressed by tumour cells in LNMBAC; thus, they could be type II pneumocyte-lineage tumour markers. We postulate that there are two main reasons why many novel type II pneumocyte lineage tumour markers were identified by this simple comparison of expression profiles. The first reason is that LNMBACs have a relatively smaller interstitial area when compared to advanced adenocarcinomas; therefore, the expression profiles mainly represent tumour cell expression. The second reason is that LNMBACs are composed of monotonous tumour cells that pathologically resemble normal type II pneumocytes. Thus, while normal lungs are composed of a mixture of type I and type II pneumocytes and bronchiolar epithelium, the comparison of expression profiles of LMNBACs and normal lungs reflected the difference in the number of 'normal and neoplastic' type II pneumocytes. The molecular signature corresponds to the histological features; the tumour cells in LNMBACs also mimic the characteristics of type II pneumocytes at the molecular level. These findings support the hypothesis that some type II pneumocytes may be progenitor cells for adenocarcinomas of the BAC type. Immunohistological analysis also revealed that some type II pneumocyte lineage markers, such as *AQP3* and *Claudin-4*, might be over-expressed by tumour cells and may have some carcinogenic function.

In summary, we analysed the gene expression profile of LNMBAC and identified novel type II lineage tumour markers in addition to a novel tumour marker, *MRP3*, whose induction reflected the stepwise progression of lung adenocarcinogenesis. This study serves as a step toward better diagnosis and treatment of LNMBAC.

Acknowledgements

This work was supported by the Programme for the Promotion of Fundamental Studies in Health Sciences of the National Institute of Biomedical Innovation (NiBio); a Grant-in-aid from the Twenty-first Century Centre of Excellence Programme and Scientific Research on Priority Areas from the Ministry of Education, Culture, Sports, Science and Technology of Japan; a Grant-in-aid from the Third Term Comprehensive 10-Year Strategy for Cancer Control from the Ministry of Health, Labour and Welfare of Japan. We are grateful to Ken Yamazaki for his excellent technical assistance.

Supplementary material

Supplementary material may be found at the web address: http://www.interscience.wiley.com/jpages/0022-3417/suppmat/path.2383.html

References

1. Yamasaki M, Takeshima, Fujii S, Matsuura M, Tagawa K, Inai K. Correlation between morphological heterogeneity and genetic alteration within one tumor in adenocarcinomas of lung. *Pathol Int* 2000;**50**:891–896.
2. Chapman AD, Kerr KM. The association between atypical adenomatous hyperplasia and lung cancer. *Br J Cancer* 2000;**83**:632–636.
3. Kitamura H, Kameda Y, Takaaki I, Hayashi H. Atypical adenomatous hyperplasia of lung. *Am J Clin Pathol* 1999;**111**:610–622.
4. Niho S, Yokose Y, Suzuki K, Kodama T, Nishiwaki Y, Mukai K. Monoclonality of atypical adenomatous hyperplasia of lung. *Am J Pathol* 1999;**154**:249–254.
5. Nakahara R, Yokose T, Nagai K, Nishiwaki Y, Ochiai A. Atypical adenomatous hyperplasia of the lung: a clinicopathological study of 118 cases including cases with multiple atypical adenomatous hyperplasias. *Thorax* 2001;**56**:302–305.
6. Nomori H, Horio H, Naruke T, Suenuma K, Morinaga S, Noguchi M. A case of multiple atypical adenomatous hyperplasia of lung detected by computer tomography. *Japan J Clin Oncol* 2001;**31**:514–516.
7. Noguchi M, Morikawa A, Kawasaki M, Matsuno Y, Yamada M, Hirohashi S, *et al*. Small adenocarcinoma of the lung. *Cancer* 1995;**75**:2844–2852.
8. Aoyagi Y, Yokose T, Minami Y, Ochiai A, Iijima T, Morishita Y, *et al*. Accumulation of losses of heterozygosity and multistep carcinogenesis in pulmonary adenocarcinoma. *Cancer Res* 2001;**61**:7950–7954.
9. Kurasono Y, Ito T, Kameda Y, Nakamura N, Kitamura H. Expression of cyclin D1, retinoblastoma gene protein, and p16 MTS1 protein in atypical adenomatous hyperplasia and adenocarcinoma of lung. *Virchows Arch* 1998;**432**:207–215.
10. Maeshima A, Sakamoto M, Hirohashi S. Mixed mucinous-type and non-mucinous-type adenocarcinoma of the lung: immunohistochemical examination and *K-ras* gene mutation. *Virchows Arch* 2002;**440**:598–603.
11. Slebos R, Baas I, Clement M, Offerhaus J, Askin F, Hruban R, *et al*. p53 alterations in atypical alveolar hyperplasia of the human lung. *Human Pathol* 1998;**29**:801–808.
12. Bhattacharjee A, Richards WG, Staunton J, Li C, Monti S, Vasa P, *et al*. Classification of human lung carcinomas by mRNA expression profiling reveals distinct adenocarcinoma subclasses. *Proc Natl Acad Sci USA* 2001;**98**:13790–13795.
13. Garber ME, Troyanskaya OG, Schluens K, Petersen S, Thaesler Z, Pacyna-Gengelbach M, *et al*. Diversity of gene expression in adenocarcinoma of the lung. *Proc Natl Acad Sci USA* 2001;**98**:13784–13789.

14. Tomida S, Koshikawa K, Yatabe Y, Harano T, Ogura N, Mitsudomi T, *et al.* Gene expression-based, individualized outcome prediction for surgically treated lung cancer patients. *Oncogene* 2004;**23**:5360–5370.
15. Chuma M, Sakamoto M, Yamazaki K, Ohta T, Ohki M, Asaka M, *et al.* Expression profiling in multistage hepatocarcinogenesis: identification of HSP70 as a molecular marker of early hepatocellular carcinoma. *Hepatology* 2003;**37**:198–207.
16. Kool M, Liden M, Haas M, Schffer GL, Vree JM, Smith AJ, *et al.* MRP3, an organic anion transporter able to transport anti-cancer drugs. *Proc Natl Acad Sci USA* 1999;**96**:6914–6919.
17. Leonard GD, Fojo T, Bates SE. The role of ABC transporters in clinical practice. *Oncologist* 2003;**8**:411–424.
18. Fukuoka-Uesaka H, Saito Y, Maekawa K, Hasegawa R, Suzuki K, Yanagawa T, *et al.* Genetic variation of the ABC transporter gene ABCC3 in a Japanese population. *Drug Metab Pharmacokinet* 2007;**22**(2):129–135.
19. Belinsky MG, Dawson PA, Shchaveleva I, Bain LJ, Wang R, Ling V, *et al.* Analysis of the *in vivo* functions of Mrp3. *Mol Pharmacol* 2005;**68**(1):160–168.
20. Oguri T, Isobe T, Fujita K, Ishikawa N, Kohno N. Association between expression of the *MRP3* gene and exposure to platinum drugs in lung cancer. *Int J Cancer* 2001;**93**:584–589.
21. Young LC, Campling BG, Cole SPC, Deeley RG, Gerlach JH. Multidrug resistance protein MRP3, MRP1, and MRP2 in lung cancer: correlation of protein levels with drug response and messenger RNA levels. *Clin Cancer Res.* 2001;**7**:1798–1804.
22. Miller VA, Hirch FA, Johnson DH. Systemic therapy of advanced bronchiolar cell carcinoma: challenges and opportunities. *J Clin Oncol.* 2005;**23**(14):3288–3293.
23. Hadnagy A, Gaboury L, Beaulieu R, Balicki D. SP analysis may be used to identify cancer stem cell populations. *Exp Cell Res* 2006;**312**(19):3701–3710.
24. Ho MM, Ng AV, Lam S, Hung JY. Side population on human lung cancer cell lines and tumors is enriched with stem-like cancer cells. *Cancer Res* 2007;**67**(10):4827–4833.
25. Fehrenbach H. Alveolar epithelial type II cell: defender of the alveolus revisited. *Respir Res* 2001;**2**:33–46.

Cytological Features of Signet-Ring Cell Carcinoma of the Lung:
Comparison With the Goblet-Cell-Type Adenocarcinoma of the Lung

Koji Tsuta, M.D.,[1] Yasuo Shibuki, C.T., I.A.C.,[1] Naoki Maezawa, C.T., I.A.C.,[1] Naobumi Tochigi, M.D.,[2] Akiko Miyagi Maeshima, M.D.,[1] Yuko Sasajima, M.D.,[1] Hisao Asamura, M.D.,[3] and Yoshihiro Matsuno, M.D.[1*]

Signet-ring cell carcinoma (SRCC) and goblet-cell-type adenocarcinoma (GCA) are mucin-producing lung adenocarcinomas. Primary SRCC shows an aggressive clinical course, whereas GCA shows infrequent distant metastasis, but more frequent intrapulmonary metastases resembling lobar pneumonia. To distinguish SRCC from GCA, this study investigated the respective cytological features of these lesions. We selected 10 cases each of SRCC and GCA from the archival imprint smears. We assessed them for the following 10 cytological features. Necrosis/debris was observed in 60% of the SRCC and 90% of the GCA. A mucinous background was observed in 10% of the SRCC and 90% of the GCA. Significant inflammation was observed in none of the SRCC and 80% of the GCA. Stromal cluster was observed in 30% of the SRCC and 70% of the GCA. Nuclear overlapping was observed in 50% of the SRCC and in all of the GCA. Single tumor cells were observed in 80% of the SRCC and 10% of the GCA. Honeycomb-like cluster was observed in none of the SRCC and 80% of the GCA. Prominent nucleolus was observed in 50% of the SRCC and 40% of the GCA. Nuclear membrane irregularity was observed in 70% of SRCC and 60% of the GCA. Nuclear pleomorphism was observed in all of the SRCC and none of the GCA. The cytological features of SRCC were the presence of single tumor cells and nuclear pleomorphism, whereas that of GCA were the presence of abundant mucin and significant inflammation in the background, and a honeycomb-like cluster. Diagn. Cytopathol. 2009;37:159–163. © 2009 Wiley-Liss, Inc.

[1]Division of Clinical Laboratory, National Cancer Center Hospital, Tokyo, Japan
[2]Pathology Division, National Cancer Center Research Institute, Tokyo, Japan
[3]Division of Thoracic surgery, National Cancer Center Hospital, Tokyo, Japan
*Correspondence to: Yoshihiro Matsuno, M.D., Division of Clinical Laboratory, National Cancer Center Hospital, 1-1 Tsukiji 5-chome, Chuo-ku, Tokyo 104-0045, Japan. E-mail: ymatsuno@med.hokudai.ac.jp
Received 27 February 2008; Accepted 16 May 2008
DOI 10.1002/dc.20897
Published online 23 January 2009 in Wiley InterScience (www.interscience.wiley.com).

Key Words: imprint smear; lung adenocarcinoma; signet-ring cell carcinoma; mucinous-bronchiolo-alveolar carcinoma

Signet-ring cell carcinoma (SRCC), a unique subtype of mucin-producing adenocarcinoma, is characterized by abundant intracellular mucin accumulation and a crescentic nucleus displaced toward one end of the cell which may arise in various organs, including the stomach, colon, urinary bladder, prostate, and breast.[1–5]

We previously reported the clinicopathological and histological characteristics of primary lung carcinoma containing SRCC components. When the SRCC component occupied 50% or more of the lesion, the age of occurrence was younger, and blood vessel invasion, lymph vessel invasion, and lymph node metastasis were significantly more frequent, and the pathological stage was higher than in carcinomas whose SRCC component occupied less than 50% of the lesion, and in the non-SRCC. Furthermore, the 5-year survival rate of patients with an SRCC component occupying 50% or more of the lesion was significantly lower (28.4%) than that of patients with an SRCC component occupying less than 50% of the lesion (50.0%), or those with a non-SRCC lesion (52.7%).[6]

Goblet-cell-type adenocarcinoma (GCA) is characterized by displacement of the nucleus to the base of tall columnar cells that contain an abundance of cytoplasmic mucin and by growth along the alveolar walls. Most GCA lesions are classified as mucinous bronchiolo-alveolar-carcinoma (BAC) in the latest WHO classification.[7] GCA is associated with less frequent lymph node and/or distant metastasis than the conventional types of adenocarcinoma, but with more frequent intrapulmonary

metastasis, showing lobar pneumonia-like clinical features.[8]

We previously analyzed the immunohistochemical differences between SRCC and GCA and compared these findings with those of normal tissue with 18 antigen expression patterns. These findings indicated that SRCC clustered as alveolar lining cells, whereas GCA clustered as gastric foveolar cells and bronchial goblet cells.[9]

Although SRCC and GCA are both mucin-producing primary lung carcinomas, each lesion exhibits distinct clinical features and immunohistochemical characteristics. The distinction of SRCC from GCA is critical because there are major differences in the clinical manifestations. The cytologic features of SRCC of the lung are not yet fully understood, because of the rarity of primary SRCC of the lung, which has incidence ranging from 0.14 to 1.9% of all lung carcinomas.[10,11] In this study, we elucidated the cytologic features of SRCC in the lung and compared these findings with those of GCA.

Materials and Methods

Cases and Tumor Specimens

We selected 10 cases each of SRCC and GCA from the archival imprint smears. Imprint smears were obtained from the maximum fresh cut surface of surgically resected tumor specimens, fixed routinely in 95% ethanol and then stained using the Papanicolaou technique. The resected specimens were then fixed in an inflated state by transbronchial infusion and/or injection of 10% buffered formalin. All tissue blocks containing tumor tissue were embedded in paraffin. Consecutive 5-μm sections were cut and then stained with hematoxylin–eosin and alcian blue–periodic acid-Schiff.

All histologic specimens were carefully evaluated by two or three certificated pathologists. None of these cases had undergone any preoperative chemotherapy or radiotherapy. The research was approved by the Institutional Review Board and an informed consent was obtained from each patient enrolled in this study.

Cytologic Examination

Imprint smear slides, three to four in each case, were examined by three observers (K. T., Y. S., and N. M.) and assessed for the following parameters without knowledge of the clinicopathologic data for each patient.

Background. The parameters included the presence or absence of (1) necrosis and/or debris, (2) mucinous background (lump of mucin or entire background), (3) significant inflammation (moderate to severe inflammatory cell infiltration), and (4) stromal cluster (myxomatous stroma with spindle cells).

Table 1. The Cytological Features of SRCC and GCA

	SRCC		*GCA*		
	(−)	*(+)*	*(−)*	*(+)*	*P* value
Necrosis and/or debris	5	5	1	9	0.141
Mucinous background	9	1	1	9	<0.001
Significant inflammation	10	0	2	8	0.001
Stromal cluster	7	3	3	7	0.179
Nuclear overlapping	4	6	0	10	0.087
Single tumor cells	2	8	9	1	0.001
Honeycomb-like cluster	10	0	2	8	0.001
Prominent nucleolus	5	5	6	4	1.000
Nuclear membrane irregularity	3	7	4	6	1.000
Nuclear pleomorphism	0	10	10	0	<0.001

SRCC, signet ring cell carcinoma; GCA, goblet cell adenocarcinoma.

Shape of the Tumor Cluster. Additional parameters included the presence or absence of (5) nuclear overlapping in more than three layers, (6) single tumor cells, and (7) a honeycomb-like cluster.

Cytomorphological Features. The parameters included the presence or absence of (8) prominent nucleolus, (9) nuclear membrane irregularity, and (10) nuclear pleomorphism (more than 3-fold variation in nuclear size).

Disagreements in judgment were resolved by means of a joint review of the slides using a multiheaded microscope.

Statistical Analysis

Statistical analysis was performed using SPSS 12.0 for Windows (SPSS, Chicago, IL). Chi-square or Fisher's exact tests were used and a P value of 0.05 or less was regarded as significant.

Results

Background

The cytological features of SRCC and GCA are shown in Table 1. The presence of necrosis and/or debris was observed in 5 of 10 SRCC (50%) (Fig. 1A) and in 9 of 10 GCA (90%) (Fig. 1B). A mucinous background was observed in 1 of 10 SRCC (10%) and 9 of 10 GCA (90%). Significant inflammation was observed in none of the SRCC and 8 of 10 GCA (80%). In GCA, the main component of the inflammatory cells consisted of polymorphonuclear leukocytes. However, in SRCC the accompanying inflammatory cells consisted of mainly a few lymphocytes. A stromal cluster was found in 3 of 10 SRCC (30%) and in 7 of 10 GCA (70%).

Shape of the Cluster

Clusters with nuclear overlapping in more than three layers were observed in 6 of 10 SRCC (60%) and all GCA (100%). The presence of single tumor cells

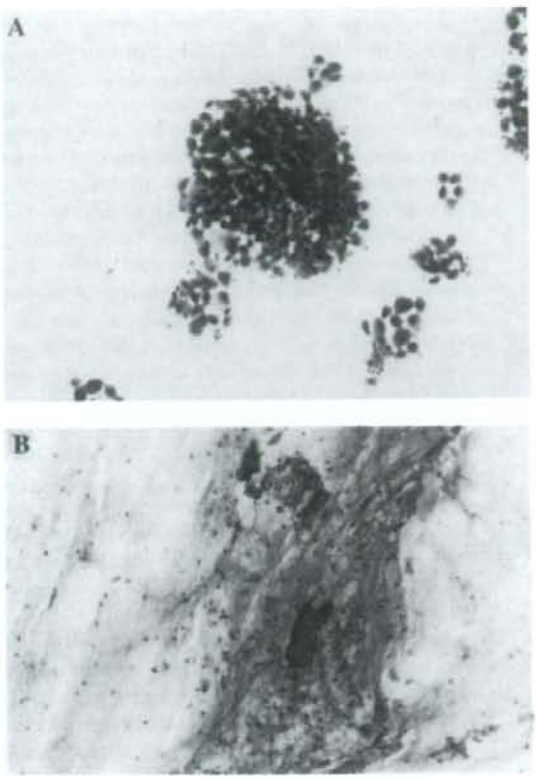

Fig. 1. A: As a cytological feature of SRCC, the tumor cluster showed a slightly loose cohesive cluster with a clear background. Papanicolaou stain, ×10. **B:** As cytological features of GCA, the tumor cluster showed tightly packed clusters with abundant mucin and inflammatory background. Papanicolaou stain, ×10. [Color figure can be viewed in the online issue, which is available at www.interscience.wiley.com.]

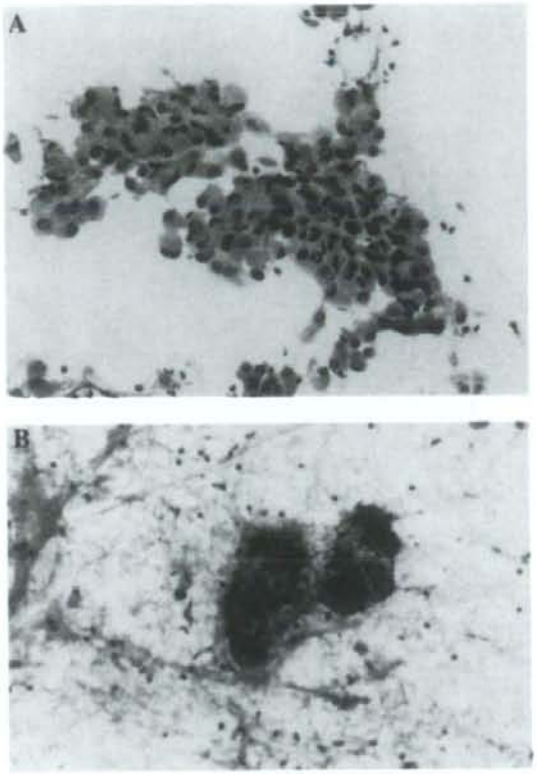

Fig. 2. A: As cytological features of SRCC, the tumor nest is partly composed of varying amounts of granular intracellular mucin accumulation and a crescentic nucleus displaced toward one end of the cell. Papanicolaou stain, ×20. **B:** As cytological features of GCA, the tumor nest is composed of abundant intracellular mucin accumulation and clear cell borders with honeycomb-like cluster. Papanicolaou stain, ×20. [Color figure can be viewed in the online issue, which is available at www.interscience.wiley.com.]

was observed in 8 of 10 SRCC (80%) (Fig. 2A) and 1 of 10 GCA (10%). A honeycomb-like cluster was observed in none of SRCC and in 8 of 10 GCA (80%) (Fig. 2B).

Cytomorphological Features

The presence of a prominent nucleolus was observed in 5 of 10 SRCC (50%) and 4 of 10 GCA (40%). The presence of nuclear membrane irregularity was observed in 7 of 10 SRCC (70%) and 6 of 10 GCA (60%). The presence of nuclear pleomorphism was observed in all SRCC (Fig. 3A) and none of the GCA (Fig. 3B).

The tumor cluster of SRCC was composed of varying amounts of mucin-containing cells. Only a few clusters were observed in which all cells consisted of mucin-containing cells. The mucin in the cytoplasm of SRCC appeared granular to pinkish. The tumor cluster of GCA consisted almost completely of mucin-containing tall columnar cells. Mucin in the cytoplasm of GCA appeared clear to yellowish.

Statistical Analysis

The statistical analysis demonstrated the cytological features of SRCC to include the presence of single tumor cells and nuclear pleomorphism. In addition, the cytological features of GCA included the presence of a mucinous background and significant inflammation, with the formation of honeycomb-like cluster.

Discussion

In this study, we elucidated and compared the cytological features of SRCC and GCA. SRCC and GCA each showed the respective characteristic cytological features. The cytological features of SRCC were the presence of single tumor cells, nuclear membrane irregularity with nuclear pleomorphism, a less mucinous background, and

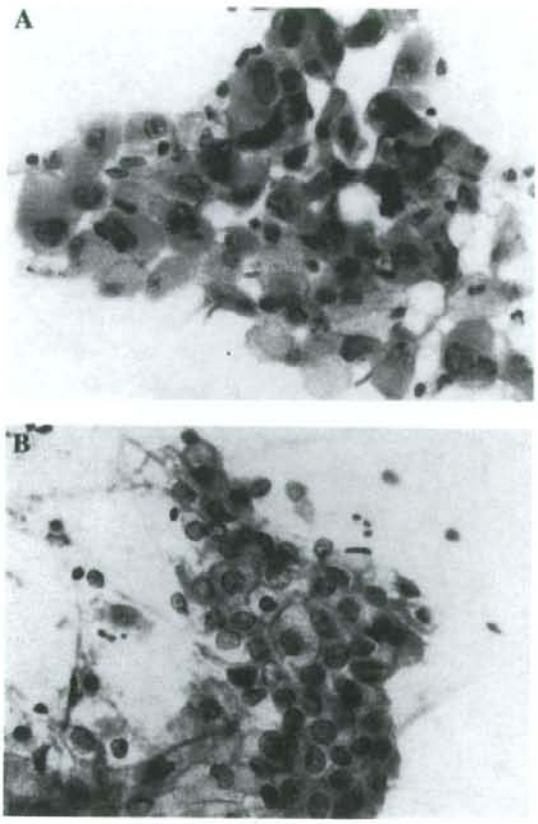

Fig. 3. A: As cytological features of SRCC, the tumor cells showed distinctive nuclear pleomorphism and prominent nucleoli. Papanicolaou stain, ×40. **B:** As a cytological feature of GCA, the tumor cells showed nuclear membrane irregularity without nuclear pleomorphism. Papanicolaou stain, ×40. [Color figure can be viewed in the online issue, which is available at www.interscience.wiley.com.]

less inflammatory cell infiltration. The cytological features of GCA were a tightly packed three-dimensional cluster with a honeycomb-like arrangement, nuclear membrane irregularity without nuclear pleomorphism, a mucinous background, and significant inflammation.

Almost all GCA showed a dirty background, thus demonstrating the presence of necrosis and/or debris, and significant inflammation. However, only half of SRCC showed a dirty background. In some organs, a dirty background indicates an invasive carcinoma. In general, GCA is known to show less invasive growth than SRCC. These differences may explain the biological reaction to excessive mucin in the background. Although, both SRCC and GCA produce and retain mucin in the cytoplasm, SRCC tends to retain mucin only in the cytoplasm, whereas GCA tends to not only retain mucin, but also to secrete mucin.

Both SRCC and GCA demonstrated nuclear membrane irregularity. However, nuclear pleomorphism was exclusively observed in SRCC. In lung adenocarcinoma, nuclear pleomorphism is known to be a predictor of invasiveness.[12,13] These findings may be related to the characteristic features of SRCC, which favor invasion of the parenchyma and promote distant metastasis.[6] Furthermore, we demonstrated that nuclear pleomorphism served as one of the criteria to differentiate SRCC and GCA.

We observed differences in the formation of tumor clusters between SRCC and GCA. Cell–cell adhesion is important for the maintenance of tissue architecture and the alteration of biologic behavior of tumor cells. Recently, Moon et al.[14] reported that SRCC of the lung showed reduced E-cadherin and β-catenin expression. E-cadherin and β-catenin complexes have been suggested to play critical roles in cancer development and progression.[15,16] The presence of single cells or a loose cohesive cluster at the periphery in the SRCC cluster may reflect the aforementioned phenomenon.

A honeycomb-like cluster was exclusively observed in GCA. An overlapping cluster and distinctive cell borders may contribute to the honeycomb-like appearance. We previously reported that nuclear overlapping in more than three layers and more than a 3-fold variation in nuclear size were found to be independent predictive factors for invasion in small-sized lung adenocarcinomas with a nonmucinous BAC component.[12] These findings indicate that the cytological features of nuclear overlapping should not be used to judge invasion in mucin-producing lung adenocarcinoma.

In GCA, most cells are mucin-containing cells, whereas SRCC lesions contain various amounts of coexisting nonmucinous cells. We previously reported that pure SRCC is rare and the average proportion of the SRCC component has been reported to be 41.4%.[6] The cytological findings obtained in this study are probably reflected in this observation.

The second edition of the WHO Histological Typing of Lung Tumors (1981) described BAC as "an adenocarcinoma in which cylindrical tumor cells grow upon the walls of preexisting alveoli." Much attention was focused on the recognition of the growth pattern (lepidic growth or not), but not on the tumor cell phenotype.[17]

During the last three decades, a number of studies have addressed issues related to the diagnosis of BAC by cytological methods.[12,13,18-25] However, most of these studies were performed before the application of the criteria described in the 1999 WHO third edition[26]; therefore, most of the studies analyzing these cytologic features lumped GCA together with nonmucinous BAC, while few reports elucidated the cytologic features of GCA. Thus, these previous descriptions of the cytological features do not always apply to GCA.

In a previous work, Tao et al.[20] divided BAC into three different types (secretory, nonsecretory, and poorly differentiated forms). The secretory type had round-to-oval nuclei with prominent nucleoli. The cytoplasm in the secretory type showed a greater abundance of foamy vacuolated cells than the nonsecretory type. In addition, the secretory type showed tightly packed cell clusters. It is thought that the cellular features of the secretory type resemble the cellular features of GCA at several points.

The limitation of this study is that our study cohort consisted of only imprint smears from the surgically resected tumor. So, some of the aforementioned cytological features may not reflect the true cytological materials (fine-needle aspiration and/or transbronchial brush/washing). The major importance of this work in the future would be to use these cytological features on true cytological materials with the same results obtained in the imprint specimens.

In summary, the cytological features of SRCC are the presence of single tumor cells and nuclear pleomorphism. The cytological features of GCA are the presence of a mucinous background and significant inflammation, and the formation of honeycomb-like cluster. These findings indicate that SRCC could be differentiated from GCA by the cytological material.

References

1. Yamashina M. A variant of early gastric carcinoma. Histologic and histochemical studies of early signet ring cell carcinomas discovered beneath preserved surface epithelium. Cancer 1986;58:1333–1339.
2. Tung SY, Wu CS, Chen PC. Primary signet ring cell carcinoma of colorectum: An age- and sex-matched controlled study. Am J Gastroenterol 1996;91:2195–2199.
3. Kitamura H, Sumikawa T, Fukuoka H, Kanisawa M. Primary signet-ring cell carcinoma of the urinary bladder. Report of two cases with histochemical studies. Acta Pathol Jpn 1985;35:675–686.
4. Randolph TL, Amin MB, Ro JY, Ayala AG. Histologic variants of adenocarcinoma and other carcinomas of prostate: Pathologic criteria and clinical significance. Mod Pathol 1997;10:612–629.
5. Frost AR, Terahata S, Yeh IT, Siegel RS, Overmoyer B, Silverberg SG. The significance of signet ring cells in infiltrating lobular carcinoma of the breast. Arch Pathol Lab Med 1995;119:64–68.
6. Tsuta K, Ishii G, Yoh K, et al. Primary lung carcinoma with signet-ring cell carcinoma components: Clinicopathological analysis of 39 cases. Am J Surg Pathol 2004;28:868–874.
7. Colby TV, Noguchi M, Henschke C, et al. Adenocarcinoma. In: Travis WD, Brambilla E, Muller-Hermelink HK, Harris CC, editors. Pathology and genetics: Tumors of the lung, pleura, thymus and heart. Lyon, France: IARC; 2004. p 35–44.
8. Gemma A, Noguchi M, Hirohashi S, et al. Clinicopathologic and immunohistochemical characteristics of goblet cell type adenocarcinoma of the lung. Acta Pathol Jpn 1991;41:737–743.
9. Tsuta K, Ishii G, Nitadori J, et al. Comparison of the immunophenotypes of signet-ring cell carcinoma, solid adenocarcinoma with mucin production, and mucinous bronchioloalveolar carcinoma of the lung characterized by the presence of cytoplasmic mucin. J Pathol 2006;209:78–87.
10. Hayashi H, Kitamura H, Nakatani Y, et al. Primary signet-ring cell carcinoma of the lung: Histochemical and immunohistochemical characterization. Hum Pathol 1999;30:378–383.
11. Kish JK, Ro JY, Ayala AG, et al. Primary mucinous adenocarcinoma of the lung with signet-ring cells: A histochemical comparison with signet-ring cell carcinomas of other sites. Hum Pathol 1989;20:1097–1102.
12. Maezawa N, Tsuta K, Shibuki Y, et al. Cytopathologic factors can predict invasion in small-sized peripheral lung adenocarcinoma with a bronchioloalveolar carcinoma component. Cancer 2006;108:488–493.
13. Morishita Y, Fukasawa M, Takeuchi M, et al. Small-sized adenocarcinoma of the lung: Cytologic characteristics and clinical behavior. Cancer 2001;93:124–131.
14. Moon KC, Cho SY, Lee HS, et al. Distinct expression patterns of E-cadherin and beta-catenin in signet ring cell carcinoma components of primary pulmonary adenocarcinoma. Arch Pathol Lab Med 2006;130:1320–1325.
15. Nollet F, Berx G, Van Roy F. The role of the E-cadherin/catenin adhesion complex in the development and progression of cancer. Mol Cell Biol Res Commun 1999;2:77–85.
16. Ilyas M, Tomlinson IP. The interactions of APC, E-cadherin and beta-catenin in tumour development and progression. J Pathol 1997; 82:128–137.
17. Shimosato Y, Sobin LH, Spencer H, et al. Histological typing of lung tumours.2nd ed. Geneva, Switzerland: World Health Organization; 1981.
18. Roger V, Nasiell M, Linden M, et al. Cytologic differential diagnosis of bronchiolo-alveolar carcinoma and bronchogenic adenocarcinoma. Acta Cytol 1976;20:303–307.
19. Silverman JF, Finley JL, Park HK, et al. Fine needle aspiration cytology of bronchioloalveolar-cell carcinoma of the lung. Acta Cytol 1985;29:887–894.
20. Tao LC, Weisbrod GL, Pearson FG, et al. Cytologic diagnosis of bronchioloalveolar carcinoma by fine-needle aspiration biopsy. Cancer 1986;57:1565–1570.
21. Lozowski W, Hajdu SI. Cytology and immunocytochemistry of bronchioloalveolar carcinoma. Acta Cytol 1987;31:717–725.
22. Auger M, Katz RL, Johnston DA. Differentiating cytological features of bronchioloalveolar carcinoma from adenocarcinoma of the lung in fine-needle aspirations: A statistical analysis of 27 cases. Diagn Cytopathol 1997;16:253–257.
23. Zaman SS, van Hoeven KH, Slott S, et al. Distinction between bronchioloalveolar carcinoma and hyperplastic pulmonary proliferations: A cytologic and morphometric analysis. Diagn Cytopathol 1997;16:396–401.
24. MacDonald LL, Yazdi HM. Fine-needle aspiration biopsy of bronchioloalveolar carcinoma. Cancer 2001;93:29–34.
25. Ohori NP, Santa Maria EL. Cytopathologic diagnosis of bronchioloalveolar carcinoma: Does it correlate with the 1999 World Health Organization definition? Am J Clin Pathol 2004;122: 44–50.
26. Travis WD, Colby TV, Corrin B, et al. World Health Organization. International histological classification of tumors: Histological typing of lung and plural tumors. Heidelberg: Springer; 1999.

Whole Genome Comparison of Allelic Imbalance between Noninvasive and Invasive Small-Sized Lung Adenocarcinomas

Hirofumi Nakanishi,[1,4] Shingo Matsumoto,[1,4] Reika Iwakawa,[1] Takashi Kohno,[1] Kenji Suzuki,[2] Koji Tsuta,[3] Yoshihiro Matsuno,[3] Masayuki Noguchi,[5] Eiji Shimizu,[4] and Jun Yokota[1]

[1]Biology Division, National Cancer Center Research Institute; [2]Thoracic Surgery Division and [5]Clinical Laboratory Division, National Cancer Center Hospital, Tokyo, Japan; [3]Division of Medical Oncology and Molecular Respirology, Faculty of Medicine, Tottori University, Tottori, Japan; and [4]Department of Pathology, Institute of Basic Medical Sciences, Graduate School of Comprehensive Human Sciences, Tsukuba University, Ibaraki, Japan

Abstract

Seventy-two small-sized (≤2 cm in diameter) lung adenocarcinomas consisting of 15 noninvasive and 57 invasive tumors were subjected to whole genome allelic imbalance (AI) scanning and mutational analysis of the *EGFR*, *KRAS*, and *TP53* genes to elucidate genetic pathways of early-stage lung adenocarcinomas. The chromosome 13q13 region showed the most frequent AI (58%) and was affected at similar frequencies between noninvasive and invasive tumors (53% and 60%, respectively), as *EGFR* and *KRAS* mutations were. The number of AI regions as well as the frequency of *TP53* mutations in invasive tumors was significantly higher than those in noninvasive ones [9.8 ± 5.6 versus 4.8 ± 2.8 (P = 0.00002) and 61% versus 13% (P = 0.001), respectively]. In particular, AIs at the chromosome 11p11-p12, 17p12-p13, and 18p11 regions in invasive tumors were significantly more frequent than those in noninvasive ones (P < 0.01). The results indicated that noninvasive tumors were developed by *EGFR*, *KRAS*, and 13q alterations and progressed to invasive ones by subsequent alterations of several tumor suppressor genes, including those on 11p11-p12, 17p12-p13, and 18p11 and *TP53*. AI at 8p21 was significantly more frequent in advanced stages (>IA) and associated with worse prognoses (P = 0.04) and, thus, would be involved in invasion and/or metastasis of adenocarcinoma cells and useful for the prediction of prognosis of patients with small-sized lung adenocarcinoma.
[Cancer Res 2009;69(4):1615–23]

Introduction

Adenocarcinoma is the most common histologic type of lung cancer, and its highly invasive and metastatic phenotypes cause poor prognosis of adenocarcinoma patients (1). The *EGFR* and *KRAS* genes are mutually exclusively mutated in lung adenocarcinomas, and inhibition of activities of these mutants led to the inhibition of adenocarcinoma cell growth (2–5). *EGFR* and *KRAS* mutations have been detected both in noninvasive and invasive adenocarcinomas (6–8); therefore, these alterations are considered to be critical for the development of lung adenocarcinomas, irrespective of their invasiveness. Recently, we showed that *p16* homozygous deletions occur at similar frequencies (~25%) in noninvasive and invasive adenocarcinomas, whereas the frequency of *p53* mutations in invasive ones was much higher than that in noninvasive ones (8). However, phenotypic diversities of adenocarcinomas cannot be explained only by accumulation of these genetic alterations. Importantly, lung adenocarcinomas have been shown to carry allelic losses at tens of chromosomal loci (9–14). Therefore, inactivation of several other tumor suppressor genes could also be involved in the development as well as progression of lung adenocarcinoma. Furthermore, the roles of those allelic losses in the development and/or progression of lung adenocarcinoma are largely unknown.

Small-sized (i.e., ≤2 cm in maximum diameter) lung adenocarcinomas are mainly in early stages and classified into six histologic types, A to F (15). Type A (localized bronchioloalveolar carcinoma) and type B (localized bronchioloalveolar carcinoma with foci of alveolar structural collapse) are noninvasive tumors, whereas type C (localized bronchioloalveolar carcinoma with foci of active fibroblastic proliferation), type D (poorly differentiated adenocarcinoma), type E (tubular adenocarcinoma), and type F (papillary adenocarcinoma with compressive and destructive growth) are invasive ones (1). Types A, B, and C show growth with replacement of bronchioloalveolar cells (replacement growth type); therefore, type A is considered to progress sequentially through type B to type C. In contrast, types D, E, and F show expansive and destructive growth (nonreplacement growth type), and their precursory noninvasive tumors are unknown. The detection of small-sized lung adenocarcinomas is increasing due to recent advances in spiral computed tomography scans (16, 17). However, even after complete resection by surgery, 20% of patients will not survive because of recurrence within 5 years (15). This implies that a subset of small-sized adenocarcinomas have already metastasized to other organs. Therefore, molecular analyses of small-sized adenocarcinomas are important not only to understand the mechanism of multistage lung carcinogenesis but also to identify molecular targets for diagnosis and therapy of patients.

Due to a limited fraction (~4%; ref. 18) and a small volume, only a limited number of small-sized adenocarcinomas have been examined for a few genetic alterations, including *EGFR*, *KRAS*, and *TP53* mutations and allelic imbalance (AI) of a few chromosomal loci (6–8, 19). However, a subset of the alterations, including *TP53* mutations, have been detected more frequently in invasive tumors than in noninvasive tumors. Therefore, it is likely that progression from noninvasive to invasive tumors is caused by accumulation of genetic alterations. Thus, a comprehensive analysis of genetic alterations in small-sized lung adenocarcinoma will give us critical information on molecular mechanisms of lung adenocarcinoma progression as well as genes involved in invasion and metastasis of

Note: Supplementary data for this article are available at Cancer Research Online (http://cancerres.aacrjournals.org/).

H. Nakanishi and S. Matsumoto contributed equally to this work.

Requests for reprints: Jun Yokota, Biology Division, National Cancer Center Research Institute, Tsukiji 5-1-1, Chuo-ku, Tokyo 104-0045, Japan. Phone: 81-3-3547-5272; Fax: 81-3-3542-0807; E-mail: jyokota@ncc.go.jp.

doi:10.1158/0008-5472.CAN-08-3218

adenocarcinoma cells. In this study, 72 small-sized adenocarcinomas, consisting of 15 noninvasive and 57 invasive tumors, were microdissected and subjected to whole genome AI scanning and mutational analysis of the *EGFR*, *KRAS*, and *TP53* genes. Based on the results, a genetic model for the development of noninvasive adenocarcinomas and their progression to invasive adenocarcinomas was depicted, and the association of genetic alterations with clinicopathologic factors was investigated.

Materials and Methods

Patients and tissues. In total, 379 patients with small-sized lung adenocarcinoma underwent curative pulmonary resections from 1993 to 2000 at the National Cancer Center Hospital, Tokyo, Japan. None of them received chemotherapy and radiotherapy before or after surgery. Tumors were pathologically diagnosed according to the tumor-node-metastasis classification (20). In 205 cases, surgical specimens fixed with methanol were available and, thus, were applicable for molecular analyses. Adenocarcinomas were classified into six histologic types: 7 type A, 18 type B, 152 type C, 17 type D, 6 type E, and 5 type F, according to the criteria of small-sized lung adenocarcinoma (15). All type A, B, and D cases and 40 of the 152 type C cases were subjected to DNA extraction. For the validation of association between genetic alterations and prognosis, additional 33 type C and 7 type D tumors were chosen from 380 patients who underwent curative pulmonary resections from 2001 to 2004 at the National Cancer Center Hospital and subjected to DNA extraction.

Cancer cells were obtained by laser capture microdissection using the PixCell Laser Capture Microdissection System (Arcturus Engineering) as previously described (6). Noncancerous lung tissues were obtained from the regions >5 cm from tumors with macroscopically normal morphology in the resected lobes of the lung. Genomic DNAs were extracted as described previously (6). Both the cancerous and noncancerous cell DNAs of sufficient amounts for this study were obtained from 72 cases: 6 type A, 9 type B, 40 type C, and 17 type D cases. This study was undertaken under the approval of the Institutional Review Board of National Cancer Center.

Mutation analysis of the *EGFR/KRAS/TP53* genes. The status of *EGFR/KRAS/TP53* mutations in 30 cases was previously reported (6, 8). Forty-two cases were newly analyzed in this study for mutations in exons 18 to 21 of the *EGFR* gene, in exons 1 to 2 of the *KRAS* gene, and in exons 4 to 8 of the *TP53* gene by genomic PCR and direct sequencing as described previously (6).

Detection of AI by SNP array analysis. AI was examined by the GeneChip Human Mapping 10K Array analysis (Affymetrix, Inc.) according to the method optimized for the analysis of a small amount of DNA samples as described previously (21). Genotype calls of tumors and normal lung tissues were obtained in 80.0% to 94.5% (88.3 ± 3.5) and 83.4% to 97.9% (94.5 ± 2.9), respectively, of the 11,037 SNP sites on the array, and 1,799 to 3,101 loci were informative for detection of AI in the tumors. When a SNP locus was called "homozygous" in tumor DNA and "heterozygous" in the corresponding normal tissue DNA, such a locus was judged as AI in the tumor. The fraction of AI for each tumor was calculated as the fraction of loci judged as AI.

Definition of AI region. AI regions were defined as follows by taking the call error into account. The fraction of error calls for each sample, calculated as the fraction of SNP loci for which normal tissue DNA was called as "homozygous" and tumor DNA as "heterozygous", were 0.0% to 8.9% (1.8 ± 2.3). The appearance of six consecutive "AI" loci by the call error was far less than 1, even for the case with the largest informative loci and the highest probability of call error [i.e., 3,101 informative loci × $(0.089)^6$ = 0.0015]. Thus, AI regions were defined by the criterion of containing at least six consecutive AI loci. Under the same criterion and by combination of SNP array data with spectral karyotyping and array-comparative genomic hybridization data, 1 of 13 (7.7%) trisomic chromosomes was judged as AI, and 14 of 215 (6.5%) AI regions were due to amplification/gain of one allele in our recent study (22). Therefore, one of allelic chromosomal segments was likely to be lost in most (>90%) of AI regions defined in this study.

Microsatellite analysis. Microsatellite markers, *D8S1116* and *D8S322*, were chosen based on the map location and allele frequency in the Japanese population.[6] One hundred picograms of DNA were used for PCR with a set of primers labeled with FAM and NED for *D8S1116* and *D8S322*, respectively. PCR products were run through a 3130xl Genetic Analyzer (Applied Biosystems) and analyzed by the GeneMapper software. A reduction >0.5 or an increase >2.0 of an allele in tumor was determined as AI.

Statistical analysis. Fisher's exact test was used to assess the association of two variables. The differences in the values of fraction of AI and in the number of AI regions between two groups were assessed by the unpaired *t* test. Association of genetic alterations with clinicopathologic characteristics was evaluated by logistic regression analysis (variables with $P \leq 0.2$ were selected). Overall survival of patients with and without genetic alterations was compared by Kaplan-Meier curves and the log-rank test. $P < 0.05$ was considered statistically significant. Statistical analysis was done using JMP software (version 5.1.1, SAS Institute, Inc.).

Results

Clinicopathologic characteristics and the status of *EGFR/KRAS/TP53* mutations. Clinicopathologic characteristics of 72 cases with small-sized lung adenocarcinomas are summarized in Table 1. Adenocarcinomas consisted of 15 noninvasive and 57 invasive tumors. These 72 tumors were of 55 replacement growth types (types A, B, and C) and of 17 nonreplacement growth types (type D). All type A, B, and D cases, whose genomic DNAs were available, in our cohort were enrolled for this study. Fourteen of the 15 noninvasive cases showed good prognoses, whereas 12 of the 17 type D cases showed them. To investigate the association of genetic alterations with prognosis, 40 type C cases consisting of all 19 cases with poor prognosis and 21 random cases with good prognosis were selected from the 152 type C cases in our cohort. Accordingly, the postoperative 5-year overall survival rate of 40 type C cases selected (53%) was considerably lower than those of all 152 type C cases (84%), and the population of advanced stages (>IA) in type C cases selected (53%) was higher than that in all type C cases (24%).

EGFR and *KRAS* mutations were detected in a mutually exclusive manner, being consistent with previous studies (5–8, 23, 24). Frequencies of *EGFR* and *KRAS* mutations were not significantly different between noninvasive tumors and invasive tumors (67%/53% and 13%/11%, respectively; $P > 0.05$). In replacement growth types (types A, B, and C), *EGFR* mutations were detected in ≥50% of the cases, whereas *KRAS* mutations were detected with lower frequencies (≤33%). *EGFR* mutations were detected at a lower frequency in nonreplacement growth types (18%) than in replacement growth types (67%), whereas *KRAS* mutations were detected at similar frequencies in both types (18%/9%). The frequency of *TP53* mutations in invasive tumors was significantly higher than that in noninvasive tumors (61%/13%; $P = 0.001$). *TP53* mutations were detected in none of type A (0%) and in a small subset of type B (22%) but in the majority of type C (53%) and type D (82%) tumors.

Frequency of AI on each chromosome arm. All 72 cases were subjected to a whole-genome AI scanning using a Human Mapping 10K Array covering 11,560 SNP sites placed at a mean interval of

[6] http://www002.upp.so-net.ne.jp/kyama-Q/MS.html

Table 1. Clinicopathologic characteristics and genetic alterations in small-sized lung adenocarcinomas

Clinicopathologic characteristics and genetic alterations*	Subset	Total	Subtype					
			Noninvasive tumors			Invasive tumors		
			All (%)	A (%)	B (%)	All (%)	C (%)	D (%)
		$n = 72$	$n = 15$	$n = 6$	$n = 9$	$n = 57$	$n = 40$	$n = 17$
Gender	Male	35 (49)	8 (53)	5 (83)	3 (33)	27 (47)	17 (42)	10 (59)
	Female	37 (51)	7 (47)	1 (17)	6 (67)	30 (53)	23 (58)	7 (41)
Smoking history	Nonsmoker	36 (50)	8 (53)	2 (33)	6 (67)	28 (49)	22 (55)	6 (35)
	Smoker	36 (50)	7 (47)	4 (67)	3 (33)	29 (51)	18 (45)	11 (65)
Pathologic stage	IA	41 (57)	15 (100)	6 (100)	9 (100)	26 (46)	19 (47)	7 (41)
	>IA	31 (43)	0 (0)	0 (0)	0 (0)	31 (54)†	21 (53)†	1 (59)†
Prognosis‡	Alive	47 (65)	14 (93)	6 (100)	8 (89)	33 (58)	21 (53)	12 (71)
	Dead	25 (35)	1 (7)	0 (0)	1 (11)	24 (42)¶	19 (47)¶	5 (29)
EGFR/KRAS§	E(+)/K(−)	40 (56)	10 (67)	3 (50)	7 (78)	30 (53)	27 (68)	3 (18)†,‖
	E(−)/K(+)	8 (11)	2 (13)	2 (33)	0 (0)	6 (11)	3 (8)	3 (18)
	E(−)/K(−)	24 (33)	3 (20)	1 (17)	2 (22)	21 (37)	10 (25)	11 (65)†,‖
TP53	Mutation(+)	37 (51)	2 (13)	0 (0)	2 (22)	35 (61)†	21 (53)†	14 (82)†,‖
	Mutation(−)	35 (49)	13 (87)	6 (100)	7 (78)	22 (39)	19 (47)	3 (18)
Fraction of AI (%)		24.2 ± 15.4	13.8 ± 8.3	11.4 ± 11.5	15.5 ± 5.5	27.0 ± 15.8¶	27.0 ± 15.7¶	26.9 ± 6.3¶
No. of AI regions		8.7 ± 5.5	4.8 ± 2.8	5.0 ± 3.5	4.7 ± 2.5	9.8 ± 5.6¶	9.9 ± 5.3¶	9.6 ± 6.3¶

*Clinicopathologic characteristics and genetic alterations are shown by the number of cases (%), and fraction of AI and the number of AI regions are shown as mean ± SD.

†$P < 0.05$ for the difference against types A + B by Fischer's exact test.

‡Postoperative 5-y overall survival.

§E(+), *EGFR* mutation (+); E(−), *EGFR* mutation (−); K(+), *KRAS* mutation (+); K(−), *KRAS* mutation (−).

‖$P < 0.05$ for the difference against type C by Fischer's exact test.

¶$P < 0.05$ for the difference against types A + B by unpaired t test.

210 kb. Fraction of AI in total cases was 24.2 ± 15.4% and was twice higher in invasive tumors than in noninvasive tumors ($P = 0.00008$; Table 1). The number of AI regions ranged from 0 to 21 (mean ± SD, 8.7 ± 5.5) and was also twice higher in invasive tumors than in noninvasive tumors ($P = 0.00002$).

At least two AI regions were mapped in all chromosome arms except five acrocentric arms; therefore, common regions of AIs among the 72 cases were defined on each chromosome arm. In total, 52 regions on 39 chromosome arms were defined as common, with two or more regions on 1p, 4q, 5p, 7p, 7q, 8p, 10p, 11p, and 16q (Supplementary Table S1). Frequencies of AI ranged from 8% to 58% (mean ± SD, 25.6 ± 11.8; Table 2). Therefore, regions with frequencies of AI more than mean + SD (37.4) were considered as being "hotspots" of AIs and those more than mean + 2SD (49.2) as being "critical regions" of AIs. There were nine hotspots of AIs, and two critical regions of AIs that were mapped to chromosomes 13q13 and 17p12-p13. The frequency of AI at 13q13 was 58% whereas that at 17p12-p13 was 56%.

In noninvasive tumors and invasive tumors, hotspots as well as critical regions of AIs were also defined based on the value of mean ± SD for the frequencies of AIs. In invasive tumors, hotspots and critical regions were further defined separately in types C and D. In noninvasive tumors, there were 11 hotspots distributed on several chromosome arms and was only one critical region at 13q13. In invasive tumors, there were nine hotspots and two critical regions mapped to 13q13 and 17p12-p13. Similarly, there were eight and seven hotspots and two and two critical regions, respectively, in types C and D. As a whole, 16 of either hotspots or critical regions were identified in total of or in each group of small-sized adenocarcinomas.

Common and differential AIs between noninvasive and invasive tumors. We next searched for regions of AI commonly and differentially affected among noninvasive, invasive, type C, and type D tumors (Table 2). Forty of the 52 regions did not show any significant differences in the frequency of AI among the subtypes. In particular, frequencies of AI in the 13q13 region were similar between noninvasive and invasive tumors (53% and 60%, respectively); therefore, 13q13 was commonly and frequently affected both in noninvasive and invasive tumors. The remaining 12 regions showed significant differences in the frequency of AI among the subtypes. For instance, frequencies of AI at 17p12-p13 in all invasive, type C, and type D tumors were significantly higher than that in noninvasive tumors ($P < 0.01$). Other 11 regions were also significantly more frequently affected by AI in invasive, type C, and/or type D tumors than in noninvasive tumors ($P < 0.05$). Particularly, differences in the frequency of AI at 18p11 and 11p11-p12 regions in type C and type D, respectively, against that in noninvasive tumors were highly significant ($P < 0.01$). In addition, two regions, 11p12 and 17q11, were significantly more frequently affected in both types of invasive tumors than in noninvasive tumors ($P < 0.05$). The other seven

regions were significantly more frequently affected in either type C or type D than in noninvasive tumors ($P < 0.05$). There were no regions that were significantly more frequently affected in noninvasive tumors than in invasive tumors or in either type C or type D tumors. In addition, regions whose frequencies of AI were significantly different between type C and type D tumors were not observed either.

Association of AIs with pathologic stage and prognosis. Nine regions on five different chromosomes showed AIs significantly more frequently in stage >IA tumors than in stage IA tumors

Table 2. Frequency of AI on each chromosome arm in small-sized lung adenocarcinomas

Chromosomal regions with AI	No. of cases (%)							
	Total		Subtype					
			Noninvasive		Invasive			
			A + B		All		C		D	
	$n = 72$		$n = 15$		$n = 57$		$n = 40$		$n = 17$	
1p21-p22	13	(18)	3	(20)	10	(18)	8	(20)	2	(12)
1p13-p21	13	(18)	3	(20)	10	(18)	8	(20)	2	(12)
1q21	13	(18)	3	(20)	10	(18)	7	(18)	3	(18)
2p22-p24	11	(15)	2	(13)	9	(16)	6	(15)	3	(18)
2q35-q37	12	(17)	2	(13)	10	(18)	9	(23)	1	(6)
3p14	24	(33)	4	(27)	20	(35)	14	(35)	6	(35)
3q11	23	(32)	4	(27)	19	(33)	13	(33)	6	(35)
4p12-p13	11	(15)	2	(13)	9	(16)	7	(18)	2	(12)
4q13	17	(24)	3	(20)	14	(25)	12	(30)	2	(12)
4q22	17	(24)	3	(20)	14	(25)	11	(28)	3	(18)
5p15	10	(14)	0	(0)	10	(18)	9	(23)	1	(6)
5p12-p13	10	(14)	2	(13)	8	(14)	7	(18)	1	(6)
5q23	23	(32)	3	(20)	20	(35)	16	(40)	4	(24)
6p11	14	(19)	0	(0)	14	(25)*,†	8	(20)	6	(35)*,†
6q22	26	(36)	4	(27)	22	(39)	14	(35)	8	(47)
7p21-p22	6	(8)	1	(7)	5	(9)	3	(8)	2	(12)
7p15	6	(8)	1	(7)	5	(9)	3	(8)	2	(12)
7q11	8	(11)	3	(20)	5	(9)	3	(8)	2	(12)
7q31-q32	8	(11)	3	(20)	5	(9)	2	(5)	3	(18)
7q33-q35	8	(11)	3	(20)	5	(9)	2	(5)	3	(18)
7q36	8	(11)	3	(20)	5	(9)	2	(5)	3	(18)
8p22-p23	31	(43)	4	(27)	27	(47)	19	(48)	8	(47)
8p21	31	(43)	4	(27)	27	(47)	20	(50)	7	(41)
8q11	27	(38)	3	(20)	24	(42)	17	(43)	7	(41)
9p22	33	(46)	4	(27)	29	(51)	19	(48)	[illegible]	[illegible]
9q12-q13	28	(39)	3	(20)	25	(44)	16	(40)	9	(53)
10p13-p14	12	(17)	2	(13)	10	(18)	6	(15)	4	(24)
10p12-p13	12	(17)	3	(20)	9	(16)	6	(15)	3	(18)
10p12	12	(17)	3	(20)	9	(16)	7	(18)	2	(12)
10p11	12	(17)	3	(20)	9	(16)	7	(18)	2	(12)
10q25-q26	16	(22)	4	(27)	12	(21)	9	(23)	3	(18)
11p12	16	(22)	0	(0)	16	(28)*,†	10	(25)*,†	6	(35)*
11p11-p12	16	(22)	0	(0)	16	(28)*,†	9	(23)	7	(41)†
11q24-q25	21	(29)	1	(7)	20	(35)*,†	15	(38)*,†	5	(29)
12p12-p13	24	(33)	2	(13)	22	(39)	16	(40)	6	(35)
12q11-q12	21	(29)	1	(7)	20	(35)	14	(35)*,†	6	(35)
13q13	[illegible]	[illegible]	[illegible]	[illegible]	[illegible]	[illegible]	[illegible]	[illegible]	8	(47)
14q21	14	(19)	1	(7)	13	(23)	7	(18)	6	(35)
15q14-q21	23	(32)	1	(7)	22	(39)*,†	16	(40)*,†	6	(35)
16p11	11	(15)	0	(0)	11	(19)	9	(23)	2	(12)
16q22	18	(25)	1	(7)	17	(30)	13	(33)	4	(24)
16q23-q24	18	(25)	1	(7)	17	(30)	13	(33)	4	(24)
17p12-p13	[illegible]	[illegible]	2	(13)	[illegible]	[illegible]†	[illegible]	[illegible]†	[illegible]	[illegible]†

(Continued on the following page)

Table 2. Frequency of AI on each chromosome arm in small-sized lung adenocarcinomas (Cont'd)

Chromosomal regions with AI	No. of cases (%)									
	Total		Subtype							
			Noninvasive		Invasive					
			A + B		All		C		D	
	n = 72		n = 15		n = 57		n = 40		n = 17	
17q11	32	(44)	2	(13)	30	(53)†	21	(53)*	9	(53)*
18p11	24	(33)	1	(7)	23	(40)*	18	(45)†	5	(29)
18q21	30	(42)	4	(27)	26	(46)	19	(48)	7	(41)
19p12-p13	20	(28)	4	(27)	16	(28)	10	(25)	6	(35)
19q12	20	(28)	4	(27)	16	(28)	10	(25)	6	(35)
20p11	20	(28)	1	(7)	19	(33)	15	(38)*	4	(24)
20q11	19	(26)	1	(7)	18	(32)	14	(35)*	4	(24)
21q11-q21	13	(18)	0	(0)	13	(23)	9	(23)	4	(24)
22q12	18	(25)	1	(7)	17	(30)	10	(25)	7	(41)*

NOTE: Frequency > mean + SD is marked by yellow, and frequency > mean + 2SD is marked by red.
*P < 0.05 for the difference against noninvasive tumors by Fischer's exact test.
†P < 0.01 for the difference against noninvasive tumors by Fischer's exact test.

(P < 0.05; Table 3). In particular, AI at 8p21 was also significantly more frequently detected in cases with poor prognosis than in cases with good prognosis (P = 0.046; Table 3). AIs of the other 51 regions as well as *EGFR*, *KRAS*, and *TP53* mutations were not associated with prognosis. The log-rank test also indicated that overall survival of cases with AI at 8p21 is worse than that without (Fig. 1; P = 0.036). Because 8p21 was defined as a hotspot of AI in both noninvasive and invasive tumors, AI at 8p21 was suggested to occur early in the development of adenocarcinoma. Therefore, it is possible that adenocarcinomas with AI at 8p21 are more aggressive than those without, even if the sizes of tumors are small. The result may indicate that AI at 8p21 could be a prognostic marker of small-sized adenocarcinomas.

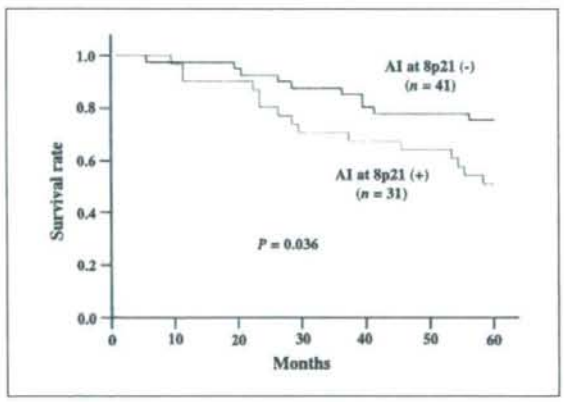

Figure 1. Prognostic significance of AI at 8p21 in patients with small-sized lung adenocarcinoma. Overall survival of patients with and without AI were compared by Kaplan-Meier curves and the log-rank test (P = 0.036).

Association of AIs with *EGFR/KRAS* mutations, gender, and smoking history. It is known that *EGFR* mutations are frequently detected in adenocarcinomas in female nonsmokers, whereas *KRAS* mutations are in adenocarcinomas in male smokers (25, 26). Such an association was also detected in this study (Supplementary Table S3). Therefore, it is important to examine whether any AIs occur in association with *EGFR/KRAS* mutations, gender, or smoking. The 72 tumors were subdivided into three groups according to the status of *EGFR/KRAS* mutations: 40 (56%) tumors with *EGFR* mutations, 8 (11%) tumors with *KRAS* mutations, and 24 (33%) tumors without *EGFR/KRAS* mutations (Table 1). Among the 52 AI regions, only 2 regions were significantly differentially affected among the three groups. 4q13 and 4q22 were more frequently affected in tumors with *EGFR* mutations than in those without *EGFR/KRAS* mutations (Supplementary Table S2). We also evaluated the association of genetic alterations with gender and smoking history. AI at 1p21-p22, 1p13-p21, and 9p22 was detected predominantly in female patients, and AI at 19p12-p13 was in smokers (Supplementary Table S3).

Genetic model for the development of lung adenocarcinoma. Based on the results, a genetic model for the development of lung adenocarcinoma was constructed (Fig. 2). Mutually exclusive *EGFR* or *KRAS* mutations were detected in the majority of type A and type B tumors, and the frequency of *EGFR/KRAS* mutations in type A and type B tumors was similar to that in type C tumors. Therefore, it is likely that type A and type B noninvasive tumors with *EGFR* or *KRAS* mutations progress to type C invasive tumors by acquisition of additional genetic alterations. A subset of type A and type B tumors had neither *EGFR* nor *KRAS* mutation and, thus, may also progress to type C invasive tumors without acquiring *EGFR* and *KRAS* mutations. The frequency of *KRAS* mutations in type D tumors was similar to those in replacement growth type (types A, B, and C) tumors, whereas the